Gut Pathogens

RESEARCH

Open Access

Exploring the role of intestinal pathogenic bacteria in metronidazole-induced bone loss: focus on *Klebsiella variicola*

Xia Chen[1,2,3,4†], Hongming Li[1,3,4†], Guang Wang[1,3,4], Zhenxing Wang[1,3,4], Yan Lv[2], Hui Xie[1,3,4*] and Sheng Zhu[1,3,4*]

Abstract

Antibiotic use is known to contribute to the development of osteoporosis, although the exact mechanisms remain poorly understood. Metronidazole (MET), a commonly prescribed antibiotic for treating anaerobic infections, has been linked to alterations in the gut microbiota (GM), which in turn are associated with various adverse side effects in the host. Recent studies have shown that the GM plays a key role in regulating bone homeostasis, though the underlying mechanisms remain under investigation. In this study, we demonstrate for the first time that MET promotes inflammatory osteoporosis through gut dysbiosis, with *Klebsiella variicola* (*K. variicola*) identified as a major pathogen influencing bone metabolism. The pro-inflammatory extracellular vesicles (EVs) secreted by *K. variicola* induce enhanced inflammatory responses and osteoclastic differentiation in both bone macrophages and bone tissue. Notably, the use of antibiotics that target *K. variicola* effectively mitigates MET-induced bone loss in vivo. This study expands our understanding of the mechanisms underlying antibiotic-induced bone loss and underscores the significant role of the pathogenic bacterium *K. variicola* in the development of osteoporosis, providing new avenues for future research on the microbiota-gut-bone axis in bone-related diseases.

Keywords Metronidazole, Gut microbiota, Osteoporosis, *Klebsiella variicola*, Extracellular vesicles

Introduction

Osteoporosis (OP), characterized by low bone mass and altered bone microstructure, affects over 200 million people globally, resulting in annual medical costs of approximately 17.9 billion dollars in USA and 37 billion euro per year in Europe [1]. Primary OP is primarily attributed to aging and postmenopausal estrogen deficiency [2]. However, more than half of patients diagnosed with osteoporosis are also associated with risk factors for secondary osteoporosis [3]. Pharmacological interventions are a significant contributor to bone loss, particularly as such treatments are often unavoidable in many clinical scenarios. Antibiotics, among the most prescribed medications worldwide, have long been used as a potent defense against infectious agents. However, their use has steadily increased to a level that raises significant concerns [4].

†Xia Chen and Hongming Li contributed equally to this work.

*Correspondence:
Hui Xie
huixie@csu.edu.cn
Sheng Zhu
zhusheng8686@csu.edu.cn
[1]Department of Orthopedics, Movement System Injury and Repair Research Center, Xiangya Hospital, Central South University, Changsha 410008, Hunan, China
[2]Department of Clinical Laboratory, Xiangya Hospital, Central South University, Changsha 410008, Hunan, China
[3]Hunan Key Laboratory of Angmedicine, Changsha 410008, Hunan, China
[4]National Clinical Research Center for Geriatric Disorders, Xiangya Hospital, Central South University, Changsha 410008, Hunan, China

In addition to fostering antibiotic resistance, which can lead to more challenging infections, prolonged antibiotic use has been implicated in the development of a variety of conditions, including asthma, allergies, obesity, and inflammatory bowel disease [5]. Previous studies have demonstrated the effects of antibiotics like penicillin and neomycin on gut microbiota and bone metabolism [6, 7], and others have reported that systemic use of multiple antibiotics increases pathogenic bacterial abundance and oral bone loss [8]. Nevertheless, the effects of different classes of antibiotics on bone metabolism and their underlying mechanisms remain poorly understood.

Notably, it has been increasingly recognized that broad-spectrum antibiotics exert a detrimental impact on the gut microbiota (GM), leading to reduced diversity, alterations in the metabolome, and disruption of gut defenses [9]. GM dysbiosis has emerged as a significant pathological mechanism in antibiotic-induced extraintestinal diseases. Recent studies have provided growing evidence that GM alterations can significantly influence bone metabolism, suggesting that the microbiota may represent a potential target for preventing bone loss [10]. Certain gut probiotics, such as *Lactobacillus* and *Akkermansia muciniphila*, have been shown to promote bone mass, while some pathogenic bacteria contribute to bone loss [11]. Consequently, it is essential to investigate whether and how GM dysbiosis mediates antibiotic-induced bone loss.

Metronidazole (MET), a widely used drug for the treatment of anaerobic infections, parasites, and certain bacterial infections, is one of the most commonly prescribed antibiotics in clinical practice [12]. MET is generally well tolerated, with reported side effects typically ranging from mild to moderate, including nausea, abdominal pain, and diarrhea [13]. Recent studies have highlighted the critical associations between MET use and gut dysbiosis. A systematic review summarizing 129 studies related to antibiotics and GM has showed that the longest duration of post-antibiotic alterations in GM was observed after treatment with MET plus clarithromycin [14]. Another study investigating the effects of different antibiotics on the human microbiome have identified that MET treatment is associated with consistent changes in GM [15]. However, no studies have established the relationship between MET treatment and osteoporosis yet. Therefore, in this study, we aimed to clarify the effects of systematic MET treatment on bone mass in skeletally mature mice and to investigate the specific mechanisms by which MET-induced GM alterations regulate bone metabolism.

Results

MET treatment induces inflammatory bone loss in mice

Three-month-old male mice were orally administered drinking water supplemented with MET and age-matched control mice were treated with plain drinking water for 8 weeks. The micro-computed tomography (μCT) analysis showed that MET treatment caused remarkable bone loss and impaired bone microstructures in the femur of mice as indicated by significantly decreased bone mineral density (BMD), trabecular bone volume fraction (Tb. BV/TV), trabecular thickness (Tb. Th), trabecular number (Tb. N), cortical thickness (Ct. Th), endocortical perimeter (Es. Pm), periosteal perimeter (Ps. Pm), and increased trabecular separation (Tb. Sp) (Fig. 1A-I). The three-point bending test indicated that MET treatment significantly reduced the maximum bending load of the tibia (Fig. 1J). Meanwhile, the Hematoxylin and eosin (H&E) staining showed that MET treatment increased inflammatory cell density in mouse bone marrow (Supplementary Figure S1A). Furthermore, the Tartrate-acid-resistant phosphatase (TRAP) staining of mouse femurs and quantitation of the number of osteoclasts (N. OCs) showed that Met treatment induced a significant increase in the number of osteoclasts (K-L). Moreover, Immunohistochemical (IHC) staining showed a significant increase in the released pro-inflammatory mediators including IL-1β and IL-6 in the bone marrow of MET-treated mice (Fig. 1M-P). Thus, oral administration of MET upregulated pro-inflammatory factors and promoted osteoclast differentiation in the bone marrow, ultimately leading to osteoporotic-like changes in mice.

MET treatment induces GM dysbiosis and caused a significant increase in klebsiella variicola abundance

We harvested and analyzed fecal samples from the MET-treated osteoporotic mice and vehicle-treated mice in order to screen for the key pathogenic bacteria contributing to MET-induced bone loss. The 16 S rRNA gene sequencing of fecal samples showed that *Enterobacteriaceae* increased most significantly at the family level after MET treatment (Fig. 2A-B). Then, the quantitative real-time polymerase chain reaction (qRT-PCR) was used to compare the abundance of the family of *Enterobacteriaceae*, and significant differences were found in the genus of *Klebsiella* (Fig. 2C-D). For there are many different species in the genus of *Klebsiella*, we conducted additional inoculations of fecal samples from MET-treated mice onto both blood agar plates and MacConkey agar plates, which aimed to discern and identify the predominant bacterial species present. The dominate bacteria with the highest number of colonies in these plates were coincident (Fig. 2E) and were identified as *Klebsiella variicola* (*K. variicola*) by a matrix-assisted laser desorption/ionization time-of-flight mass spectrometry

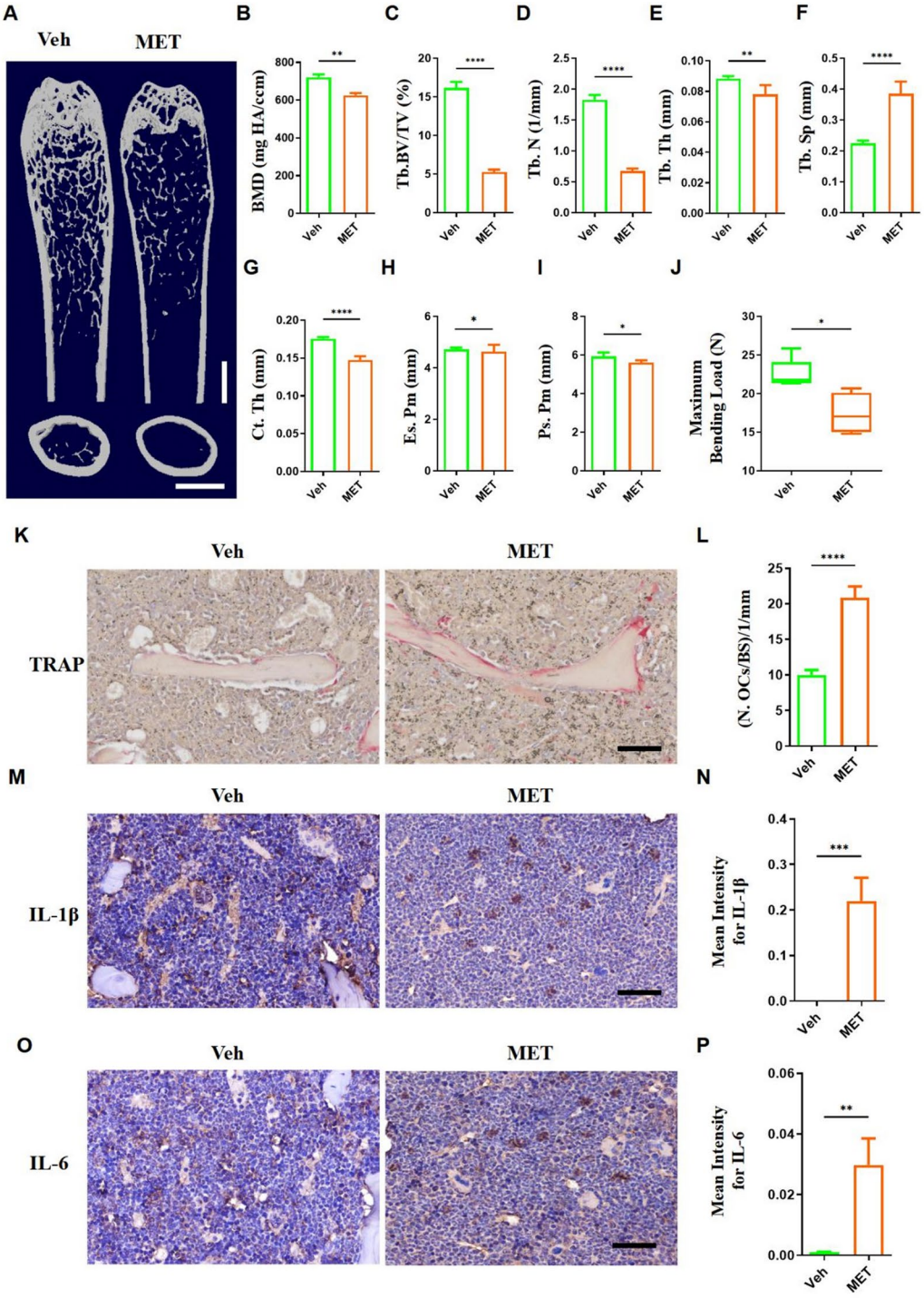

Fig. 1 Oral gavage of MET induces inflammatory bone loss in mice. (**A**) Representative μCT images of trabecular (up) and cortical (bottom) bone of femora in Veh and Met groups, Scale bar = 500 μm (Above) and 1 mm (bottom), *n* = 12; (**B**) Bone mineral density (BMD) of femora in Veh and Met groups, *n* = 6; (C-I) Quantitative μCT analysis of bone mass and microstructure. (**C**) Tb. BV/TV: trabecular bone volume fraction; (**D**) Tb. N: number of bone trabeculae; (**E**) Tb. Th: thickness of bone trabeculae; (**F**) Tb. Sp: bone trabecular separation; (**G**) Ct. Th: cortical thickness; (**H**) Es. Pm: endocortical perimeter; (**I**) Ps. Pm: periosteal perimeter; (**J**) Three-point bending measurement of tibia ultimate load, *n* = 6; (**K**) Representative images of TRAP staining, Scale bars = 100 μm, *n* = 6; (**L**) quantitation of the number of osteoclasts (N. OCs); (**M**) Representative images of immunohistochemical staining for IL-1β. Scale bars = 100 μm, *n* = 6; (**N**) quantification of mean intensity for IL-1β; (**O**) Representative images of immunohistochemical staining for IL-6, Scale bars = 100 μm, *n* = 6; (**P**) Quantification of mean intensity for IL-6

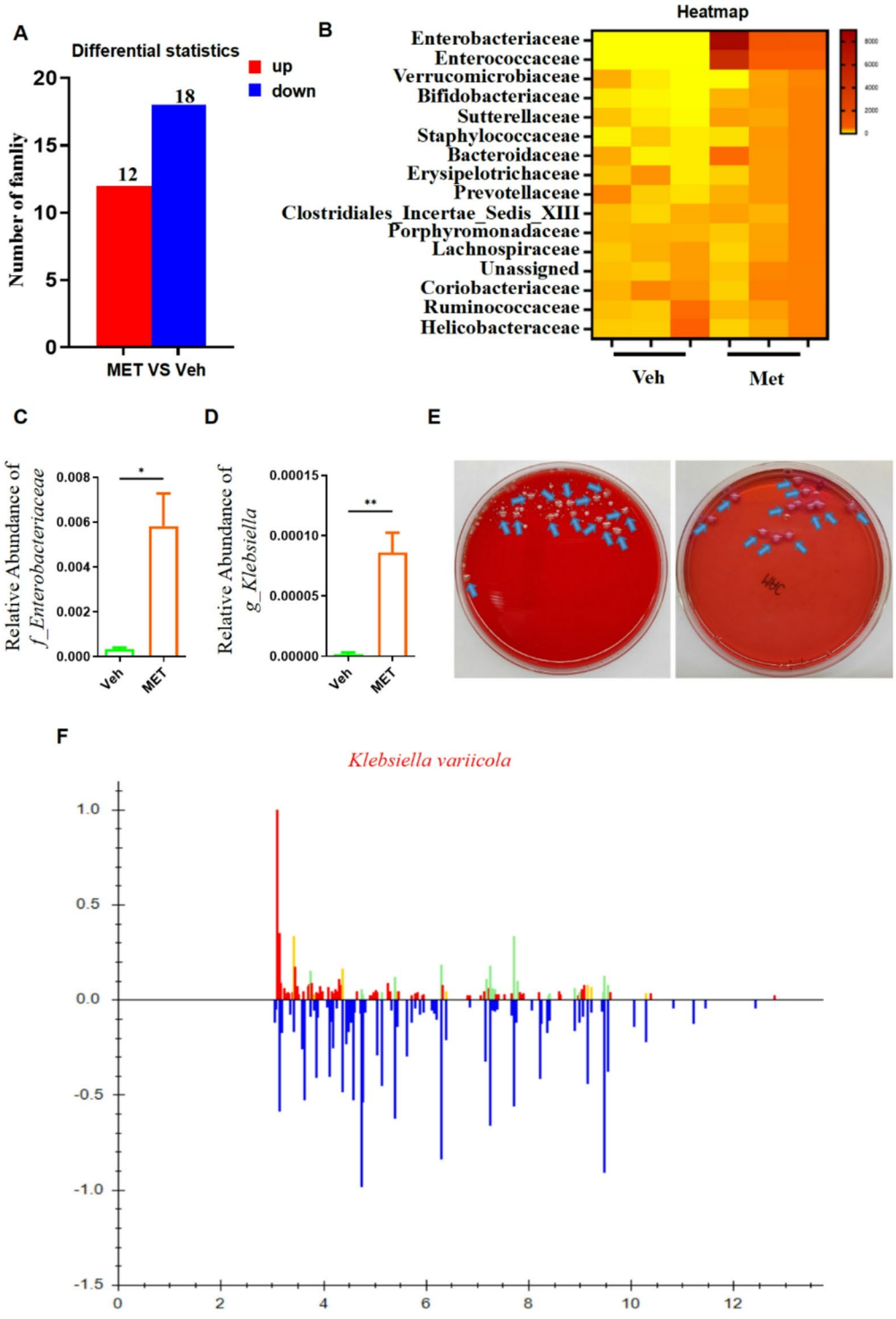

Fig. 2 Oral gavage of metronidazole induces intestinal microbiota disorder and abnormal proliferation of Enterobacteriaceae. (**A**) Histogram of fecal microbiota at the family level in Vet and MET groups tested by 16 S rRNA gene sequencing. (**B**) Heatmap of up-regulated fecal microbiota at the family lever in Vet and MET groups tested by 16 S rRNA gene sequencing; (**C-D**) qRT-PCR analysis of f_ *Enterobacteriaceae* and g_ *Klebsiella* abundance; (**E**) Bacteria cultured by blood plate and MAC plate; (**F**) Identification of main colonies in **G** (blue arrow marked) by Bruker MALDI Biotyper

(MALDI-TOF MS) with a high credibility score (Fig. 2F). Notably, increased inflammatory responses were not observed in the colonic tissues of mice treated with MET, suggesting that MET stimulation on bone marrow inflammatory responses may act through specific inflammatory mediators (Fig S2).

K. variicola transplantation induces inflammatory bone loss in mice

The abundance of *K. variicola* was significantly increased in MET-induced osteoporotic mice, but the relationship between *K. variicola* and skeletal diseases has not been reported. To examine the potential of *K. variicola* to mediate MET-induced osteoporosis, mice were transplanted with *K. variicola* by oral gavage once a week for 8 weeks. The μCT results showed that *K. variicola* transplantation led to a significant decrease of BMD, Tb. BV/TV, Tb. Th, Ct. Th and Tb. N, and increased Tb. Sp, but Es. Pm and Ps. Pm did not have statistically significant difference (Fig. 3A-I). The three-point bending test indicated that *K. variicola* transplantation reduced the maximum bending load of the tibia (Fig. 3J). Consistent with MET-treated mice, compared to Vehicle-treated mice, the number of osteoclasts and expression of pro-inflammatory factors were significantly increased in the bone marrow of *K. variicola* treated mice according to TRAP and IHC staining results. (Fig. 3K-P). These results suggested that intestinal *K. variicola* could independently induce inflammatory bone loss in vivo.

Extracellular vesicles (EVs) of K. variicola triggers inflammatory responses and osteoclastic differentiation of macrophages in vitro

As a part of the communication process between organisms, the gut microbiota produces small bodies, called microbial EVs. EVs act as shuttles for transferring bioactive cargoes (i.e., proteins, mRNAs, miRNAs, DNA, carbohydrates, and lipids) to exert efficient regulatory effects on various organs of the host [16]. Therefore, we next isolated EVs from *K. variicola* (*K. var*-EVs), and investigated their direct effects on inflammatory activation and osteoclastogenesis in macrophage lineages in vitro (Fig. 4A-B). As evidenced by the TRAP staining, *K. var*-EVs dramatically promoted the osteoclastic differentiation in bone macrophages (Fig. 4C-D). The qRT-PCR results showed that *K. var*-EVs upregulated the expression of IL-1β and IL-6 in a dose-dependent manner (Fig. 4E-F). Therefore, *K. var*-EVs exhibited the capacity to induce the inflammatory response in bone cells and to promote osteoclast differentiation.

K. var-EVs intervention induces inflammatory bone loss in vivo

Given the findings in vitro that *K. var*-EVs promoted inflammatory responses and osteoclastic differentiation, we further evaluated the effects of *K. var*-EVs on bone mass in mice. Our previous studies have demonstrated that bacterial extracellular vesicles can be translocated to bone tissue and mediate GM regulation of bone metabolism [17]. Similarly, we administered gavage of *K. var*-EVs to wild-type mice for 8 weeks. Surprisingly, significant bone loss, impaired bone microstructures and decreased bone strength were observed in *K. var*-EVs-treated mice according to the micro-CT, BMD and biomechanical test results (Fig. 5A-J). The TRAP staining results showed that *K. var*-EVs increased cell numbers of osteoclasts and the IHC staining results showed that *K. var*-EVs caused increased expression of inflammatory cytokines comparable to *K. variicola* transplantation in mice (Fig. 5K-P).

Suppression of K. variicola using Ciprofloxacin (CIP) effectively attenuates MET-induced inflammatory osteoporosis in mice

CIP is a long-used antibiotic that is effective in treating a variety of gram-negative bacterial infections. CIP has been reported to be more effective in treating Klebsiella than other common antibiotics [17]. To confirm the key role of *K. variicola* in contributing to MET-induced osteoporosis, we further intervened with CIP in MET-treated mice. Antibiotic susceptibility testing confirmed the susceptibility of *K. variicola* to CIP (Supplementary Figure S3A). The 16s rRNA sequencing of mouse feces showed that CIP intervention significantly suppressed the enhanced abundance of *Enterobacteriaceae* including *K. variicola* caused by MET (Supplementary Figure S3B). Surprisingly, CIP significantly attenuated bone loss caused by MET as measured by μCT BMD and biomechanical tests (Fig. 6A-J). Moreover, CIP intervention inhibited osteoclast numbers (Fig. 6K-L) and downregulated the expression of pro-inflammatory cytokines in bone marrow in MET-treated mice (Fig. 6M-P). These results further demonstrate the critical role of K.V bacteria in MET-induced bone loss (Fig. 7).

Discussion

The pathogenesis of osteoporosis is complex and has not yet been fully elucidated. In recent years, the microbiota-gut-bone axis has attracted increasing attention in the field of bone health. The proposal of bone microbiology has led researchers to emphasize the role of altered gut microbiome in the development of osteoporosis [18]. Sjögren et al. have shown that Germ-free mice exhibit increased bone mass associated with reduced number of osteoclasts per bone surface compared with conventionally raised mice [19]. Similarly, it has been observed

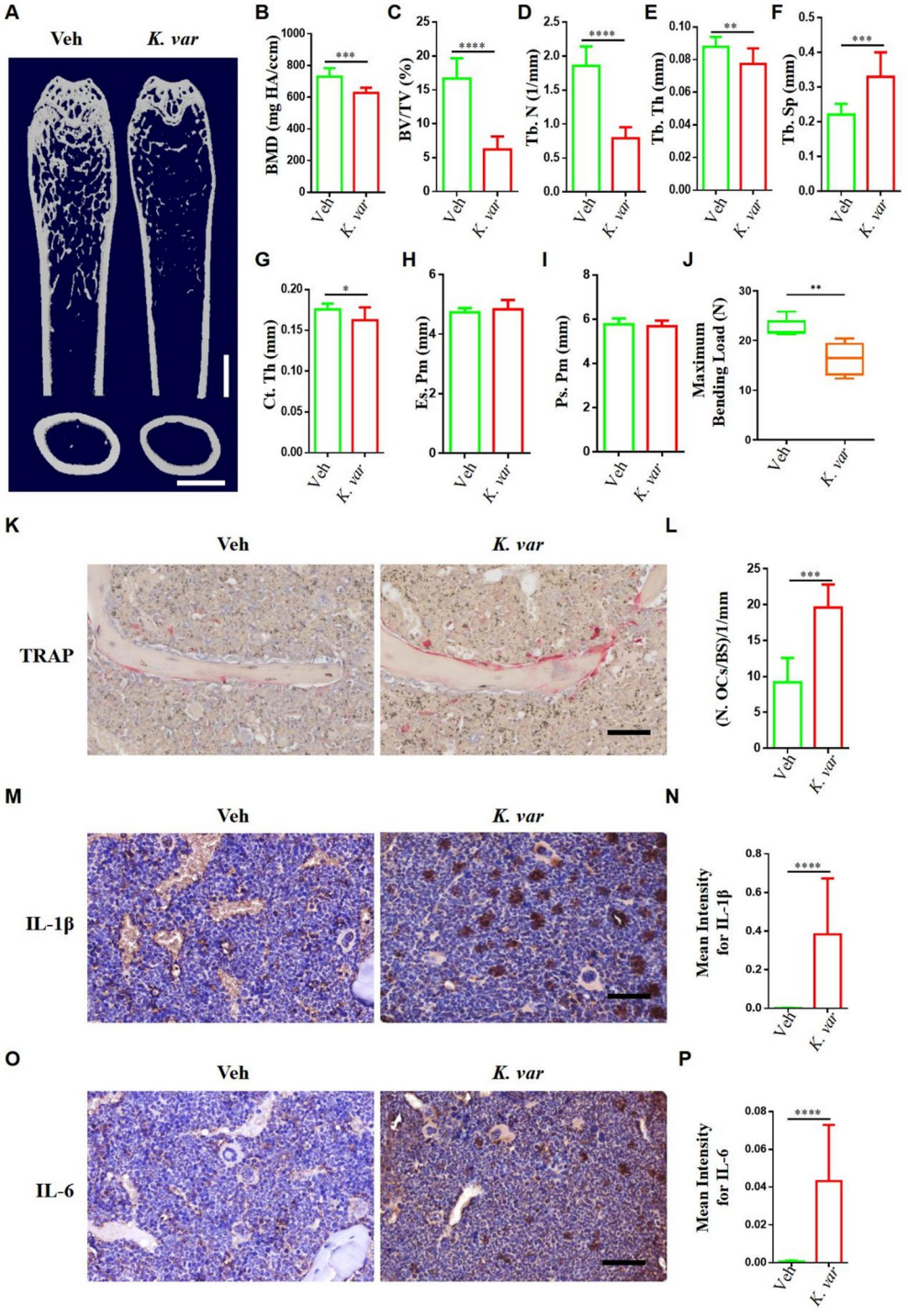

Fig. 3 *K. variicol*a transplantation induces inflammatory bone loss in mice. (**A**) Representative μCT images of trabecular (up) and cortical (bottom) bone of femora in Veh and *K. variicola* groups, Scale bar = 500 μm (Above) and 1 mm (bottom); (**B**) BMD of femora in Veh and *K. variicola* groups, *n* = 6; (**C-I**) Quantitative analysis of Tb.BV/TV, Tb. N, Tb. Th, Tb. Sp, Ct. Th, Es. Pm and Ps. Pm, *n* = 12; (**J**) Three -point bending measurement of tibia ultimate load in Veh and *K. variicola* groups, *n* = 6; (**K**) Representative TRAP -stained images of femora from mice in Veh and *K. variicola* groups, Scale bars = 100 μm; (**L**) Quantitation of the number of osteoclasts (N. OCs), *n* = 6; (**M**) Representative immunohistochemical staining images of femora from mice in Veh and *K. variicola* groups for IL-1β. Scale bars = 100 μm; (**N**) Quantification of mean intensity for IL-1β, *n* = 6; (**O**) Representative immunohistochemical staining images of femora from mice in Veh and *K. variicola* groups for IL-6, Scale bars = 100 μm; (**P**) Quantification of mean intensity for IL-6, *n* = 6

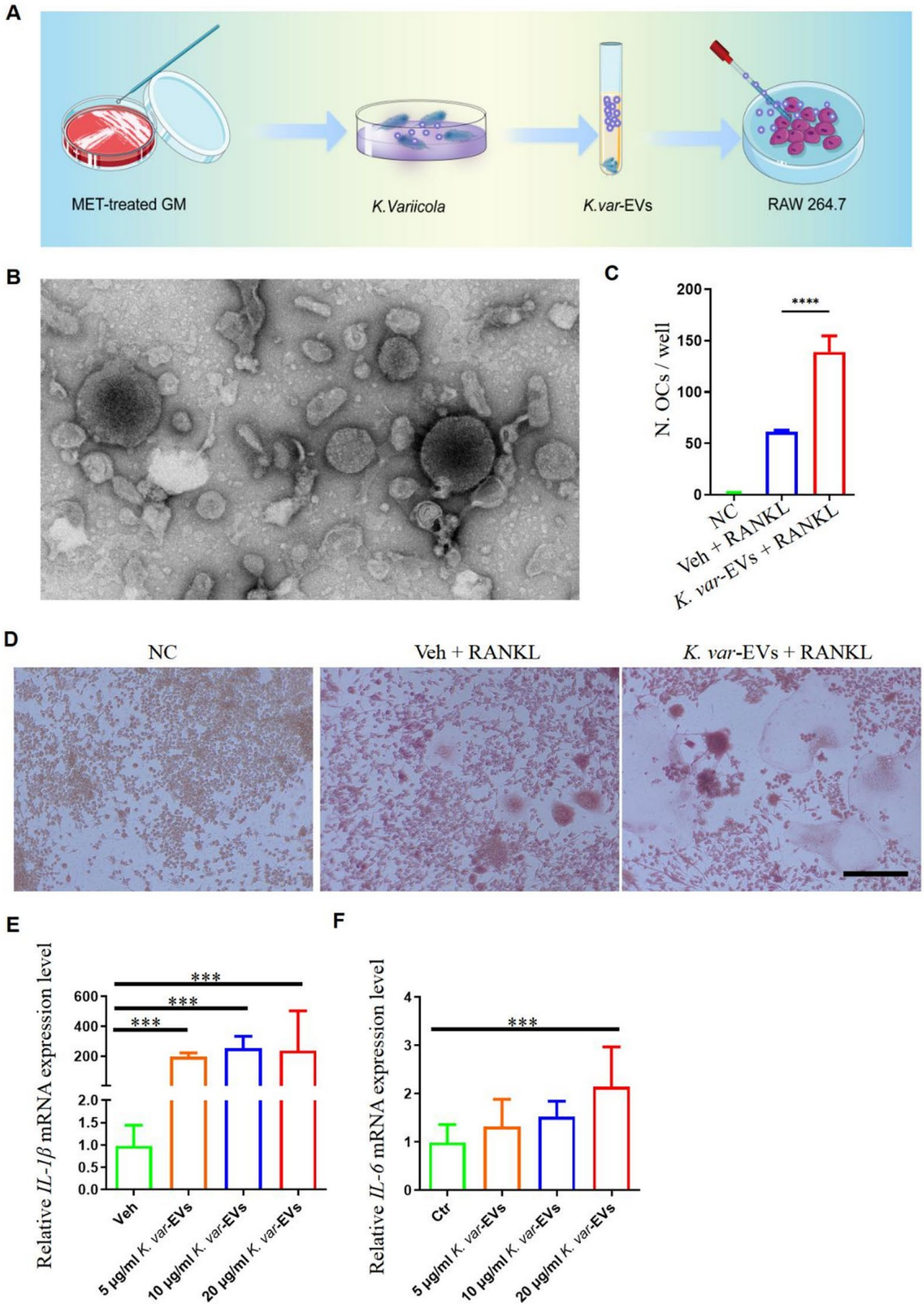

Fig. 4 *K. var*-EVs induces RAW264.7osteoclast differentiation and inflammatory response in vitro. (**A**) Schematic diagram of *K. var*-EVs isolation and its effect on RAW264.7; (**B**) Morphology of *K. var*-EVs under a transmission electron microscope. Scale bar = 50 nm; (**C**) Representative TRAP staining images of RAW264.7 cells receiving *K. var*-EVs treatment and (**D**) quantification of osteoclast number per well in a 48-well plate. Scale bar: 100 μm, $n = 5$; (**E**) and (**F**) qRT-PCR analysis of IL-1β and IL-6 mRNA relative expression level in RAW264.7 cells receiving ***K****. var*-EVs treatment, $n = 5$

that germ-free mice have relatively fewer osteoclasts and significantly less T cells and osteoclast precursors in vitro [20]. Interestingly, multiple studies have shown that supplementation with intestinal probiotics can be effective against osteoporosis in mice, such as Lactobacillus reuteri and Lactobacillus rhamnosus [21, 22]. We have previously demonstrated the efficacy of the probiotic *Akkermansia muciniphila* against postmenopausal

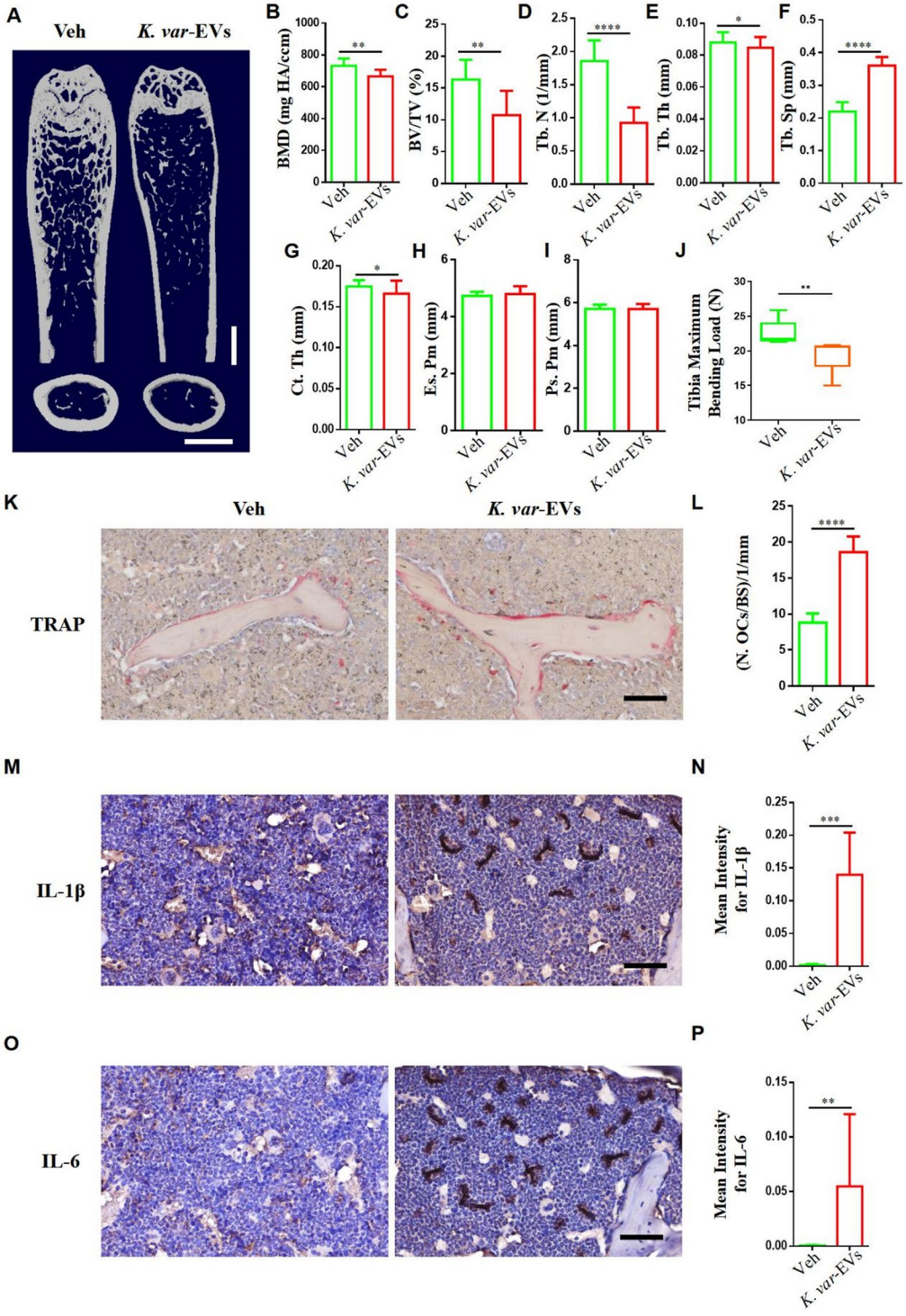

Fig. 5 *K. var*-EVs induces inflammatory bone loss in mice. (**A**) Representative μCT images of trabecular (up) and cortical (bottom) bone of femora in Veh and *K. var*-EVs groups, Scale bar = 500 μm (Above) and 1 mm (bottom), $n = 12$; (**B**) BMD of femora in Veh and *K. var*-EVs groups, $n = 6$; (**C-I**) Quantitative analysis of BV/TV, Tb. N, Tb. Th, Tb. Sp, Ct. Th, Es. Pm and Ps. Pm; (**J**) Three-point bending measurement of tibia ultimate load in Veh and *K. var*-EVs groups, $n = 6$; (**L**) Representative TRAP -stained images of femora from mice in Veh and *K. var*-EVs groups, Scale bars = 100 μm; (M) quantitation of the number of osteoclasts (N. OCs), $n = 6$; (**N**) Representative immunohistochemical staining images of femora from mice in Veh and *K. var*-EVs groups for IL-1β. Scale bars = 100 μm; (**O**) Quantification of mean intensity for IL-1β, $n = 6$; (**P**) Representative immunohistochemical staining images of femora from mice in Veh and *K. var*-EVs groups for IL-6, Scale bars = 100 μm; (**Q**) Quantification of mean intensity for IL-6, $n = 6$

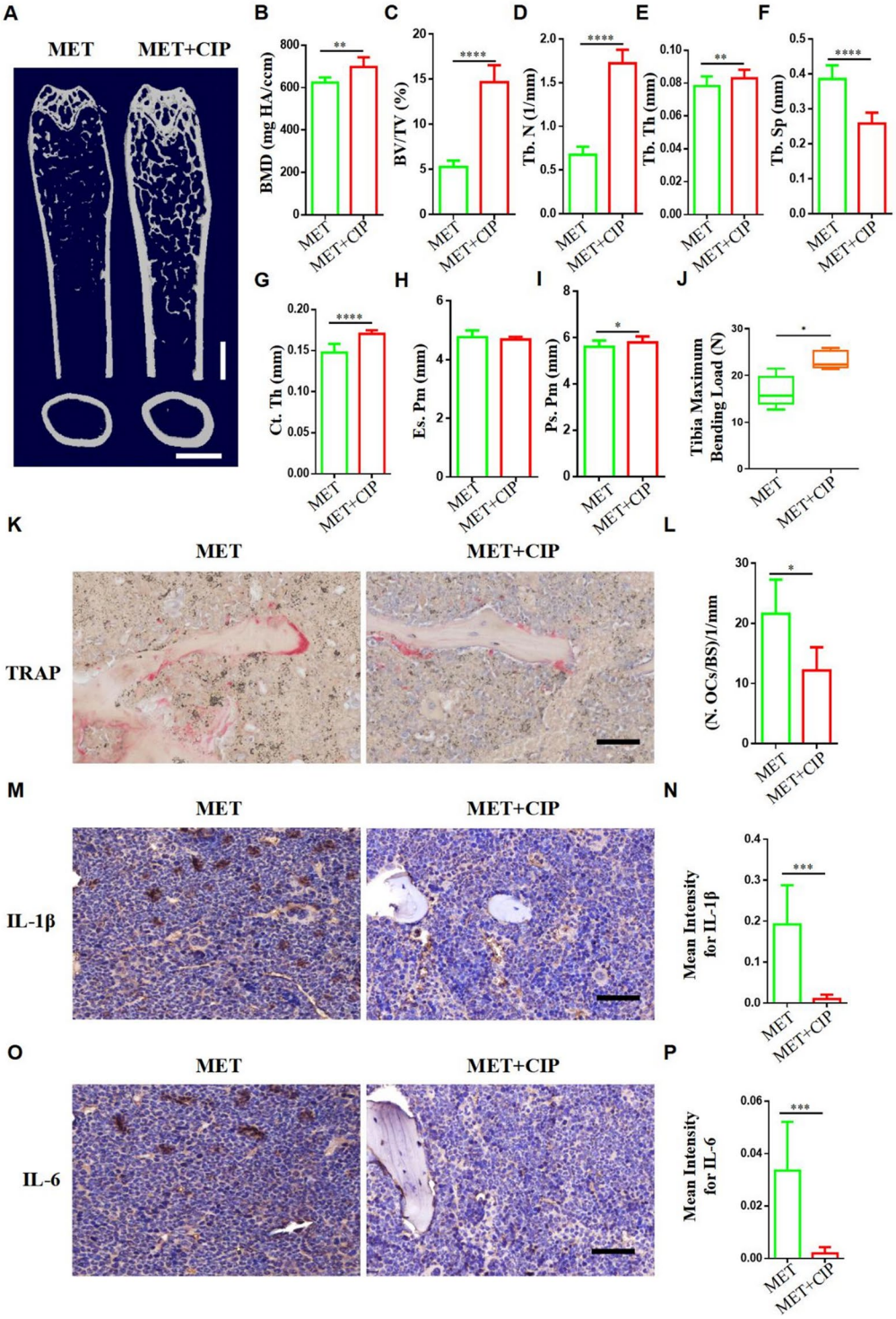

Fig. 6 CIP attenuates the MET-induced osteoporotic phenotypes. (**A**) Representative μCT images of trabecular (up) and cortical (bottom) bone of femora in MET and MET + CIP groups, Scale bar = 500 μm (Above) and 1 mm (bottom), $n = 12$; (**B**) BMD of femora in MET and MET + CIP groups, $n = 6$; (**C-I**) Quantitative analysis of BV/TV, Tb. N, Tb. Th, Tb. Sp, Ct. Th, Es. Pm and Ps. Pm; (**J**) Three-point bending measurement of tibia ultimate load in MET and MET + CIP groups, $n = 6$; (**K**) Representative TRAP -stained images of femora from mice in MET and MET + CIP groups, Scale bars = 100 μm; **(L)** Quantitation of the number of osteoclasts (N. OCs), $n = 6$; (M) Representative immunohistochemical staining images of femora from mice in MET and MET + CIP groups for IL-1β. Scale bars = 100 μm; (**N**) Quantification of mean intensity for IL-1β, $n = 6$; (**O**) Representative immunohistochemical staining images of femora from mice in MET and MET + CIP groups for IL-6, Scale bars = 100 μm; (**P**) Quantification of mean intensity for IL-6, $n = 6$

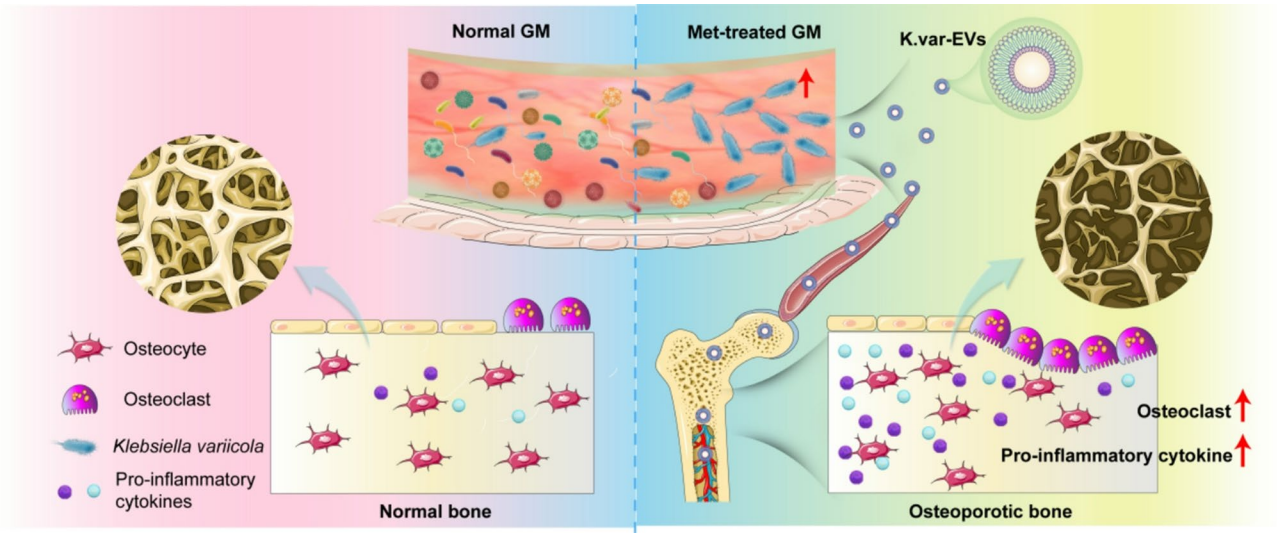

Fig. 7 Schematic diagram. Extracellular vesicles (EVs) derived from *Klebsiella variicola* excerbate inflammatory bone loss under conditions of antibiotic-induced intestinal dysbiosis

osteoporosis by analyzing differences in the GM of young children and older adults [17]. Thus, the GM has been recognized to have a significant impact on bone metabolism and to be an emerging therapeutic target for osteoporosis, but the specific regulatory bacterial species and their molecular mechanisms remain to be thoroughly explored (Fig. 7).

Antibiotics have saved the lives of countless people suffering from infectious diseases and extending the average human lifespan by more than 10 years. However, scientists have discovered that antibiotics can adversely affect the GM over the past two decades, whereby some beneficial bacteria are eliminated and the metabolic activity of other deleterious bacteria is increased [9]. It has been reported antibiotic-induced dysbiosis to be associated with obesity, diabetes, and intestinal inflammation-related diseases [16]. Limited studies have reported the effects of beta-lactam antibiotics that are effective against numerous gram-positive bacteria on bone mass. Low doses of penicillin from birth to weaning was demonstrated to increase bone mass in adult mice [23], while trabecular bone density was significantly reduced in mice treated with ampicillin and neomycin for 4 weeks due to post-antibiotic gut dysbiosis [24]. MET is a first-line clinical class of antibiotics with broad-spectrum activity against anaerobic bacteria and protozoa, and its effects on bone metabolism are unclear. Here, we have for the first time showed that MET treatment caused remarkable bone loss, impaired bone microstructures and increased bone fragility in mice. Moreover, MET treatment promoted bone loss mainly due to the induction of inflammatory response in bone marrow and the promotion of osteoclastic differentiation.

The involvement of MET in disease development through altered GM has been reported in multiple studies. It has been proposed that MET may exert a positive effect on inflammatory bowel disease and endometriosis by modulating the GM [25, 26]. Therefore, we further screened for key pathogenic bacteria by analyzing GM from MET-induced osteoporotic mice. Using 16s rRNA sequencing analysis and qRT-PCR, we identified a significant increase in the genus of *Klebsiella* in the feces of MET-treated mice. We further screened the dominant bacterial species with bacterial agar plate culture test of fecal samples and identified them as *K. variicola* by MALDI-TOF MS, which was a generally accepted method for bacterial identification [27].

K. variicola is a Gram-negative, partially anaerobic, non-motile bacillus and its infections have been reported in human worldwide [27]. *K. variicola* is increasingly recognized as an emerging human pathogen and related to infections associated with some comorbidities such as systemic lupus erythematosus, cancer, diabetes mellitus, and hepatobiliary diseases [28]. As a novel pathogen identified in recent years, its relationship with the skeletal system is obscure. In this study, to verify that K. variicola is the main pathogen of MET-induced osteoporosis, we transplanted K. variicola into skeletally mature mice and observed its effects on bone metabolism. Surprisingly, *K. variicola* transplantation resulted in similar bone loss, impaired bone microarchitecture, and increased bone fragility as in MET-treated mice.

A rising number of studies have confirmed that bacterial EVs can act as biological shuttle systems to deliver virulence factors into host cells, thereby modulating host signaling pathways and cellular processes [29]. In our previous work, we have revealed a novel mode of

gut-bone axis regulation mediated by EVs of intestinal bacteria [17]. Specifically, the regulatory effects of GM on bone metabolism require the secretion of bacterial EVs, which are nanovesicles that can enter and accumulate in bone tissue to influence osteoblastic and osteoclastic differentiation. Another study reported the role of periodontal pathogen-derived EVs in systemic bone loss and demonstrated in vivo and in vitro that they increase osteoclastogenesis and bone resorption [30]. Therefore, we have also tested the effect of EVs extracted from *K. variicola* on bone metabolism and found that mice intervened by *K.var*-EVs similarly exhibited obvious osteoporosis-like alterations. To this point, we have tentatively demonstrated the fact that MET increases the abundance of intestinal *K. variicola* and contributes to inflammatory osteoporosis, and revealed a potential mechanism by which *K. variicola* releases pro-inflammatory and pro-osteoclastic EVs to induce bone loss.

CIP is a second-generation fluoroquinolone chemosynthetic broad-acting antibiotic that fights a wide range of pathogenic bacteria including *Klebsiella*[31]. In a recent study, most of the 55 *K. variicola* isolates tested were sensitive to CIP [32]. The antimicrobial susceptibility test we performed also revealed strong anti-K. variicola activity of CIP. Therefore, we tested whether the application of CIP could counteract the increase in intestinal *K. variicola* and bone loss in MET-treated mice. As expected, CIP significantly suppressed intestinal *K. variicola* in MET-treated mice according to 16s rRNA sequencing results. Surprisingly, CIP intervention effectively downregulated bone marrow pro-inflammatory cytokines and reduced osteoclast numbers, resulting in improvement of bone mass and bone strength compared to MET-treated mice. Our findings further validate *K. variicola* as a major pathogen of MET affecting bone metabolism and provide a promising target for intervention to prevent MET-induced bone loss.

While this study provides novel insights into MET-induced osteoporosis and the pathogenic role of K. var-EVs., several limitations should be acknowledged: (1) While ciprofloxacin mitigated MET-induced bone loss, exploring non-antibiotic strategies (e.g., dietary regimens, probiotics like *Akkermansia muciniphila*, or EV-targeting prebiotics) to selectively suppress *K. variicola* without worsening dysbiosis could enhance translational impact, which is a critical concern for chronic antibiotic users. (2) While our functional assays establish the causal role of K. var-EVs in osteoclast activation, we need further investigate the precise molecular mechanisms by which K. V-derived EVs contribute to bone loss, and the key bioactive components within EVs responsible for bone loss. (3) Further validation is required in large-animal models (e.g., porcine models) and clinical cohort studies.

In conclusion, we have demonstrated for the first time that MET promotes inflammatory osteoporosis by inducing gut dysbiosis and highlighted intestinal *K. variicola* as a major pathogen affecting bone metabolism. The pro-inflammatory EVs secreted by *K. variicola* can be translocated to the bone tissue, leading to an enhanced osteoclastic differentiation. This study broadens the mechanism of antibiotic-induced bone loss and reveals the critical role of *K. variicola* in triggering bone marrow inflammatory responses and promoting osteoclastic differentiation through the secretion of *K. var*-EVs. Inhibition of specific intestinal pathogens and their functional EVs provide new targets for the prevention of antibiotic-induced osteoporosis as well as new ideas for future studies related to the microbiota-gut-bone axis.

Materials and methods

Animals and treatments

The animal care and experimental procedures were conducted in accordance with the guidelines and regulations of the Ethical Review Board at Xiangya Hospital of Central South University. Male C57BL/6J mice, aged two or three months and weighing between 20 and 24 g, were employed in this study. Mice were randomly assigned to various treatment groups. Exclusion criteria for mice included a body weight of < 18 or > 26 g or poor physical condition prior to treatment initiation. All mice were housed in specific pathogen-free conditions.

Metronidazole (Solarbio) was administered in the drinking water at a concentration of 1 g/L for a duration of 8 weeks, with mice receiving the vehicle under the same treatment regimen serving as the healthy controls. Fecal samples from MET-treated mice were collected at the 4th week of treatment for 16 S rRNA gene sequencing. To assess the impact of *K. variicola* and *K. var*-EVs, mice were orally gavaged with *K. variicola* (10^6 CFUs in 200 µl of PBS) and *K. var*-EVs (100 µg in 200 µl of PBS), or an equal volume of PBS, once a week. For therapeutic intervention, ciprofloxacin (Solarbio) was added to the drinking water at a concentration of 0.25 g/L for MET-treated mice. The femurs of ten mice from each group were collected and processed for downstream analyses after 8 weeks of treatment.

µCT analysis

After being fixed in 4% paraformaldehyde (PFA) for 2 days, the right femoral samples were analyzed with high-resolution µCT (Skyscan 1176) as described previously [33]. The scanner parameters were set to a voltage of 50 kV, a current of 400 µA, and a resolution of 11.4 µm per pixel, respectively. The analysis of femoral parameters, including Tb. BV/TV, Tb. Th, Tb. N, Tb. Sp, Ct.Th, Es.Pm, Ps.Pm, was conducted using image reconstruction software (NRecon), data analysis software (CTAn

v1.11), and three-dimensional model visualization software (μCTVol v2.2).

16s rRNA sequencing

Following the collection of fecal samples from mice subjected to vehicle, MET, or CIP + MET treatments, 16 S rRNA sequencing was conducted by GeneSky Biological Technology (Shanghai, China), including DNA extraction, PCR amplification, purification, library preparation, sequencing, bioinformatics analysis and statistical analysis.

Histological examination and immunohistochemistry

For histological and immunohistochemical analyses, femurs were embedded in 4% paraformaldehyde (PFA) for 2 days, followed by decalcification in 0.5 M EDTA for 1 week. Subsequently, the specimens underwent dehydration using graded ethanol and immersion in xylene. The specimens were then embedded in paraffin, cut into 5-μm-thick sections, and subjected to Hematoxylin and Eosin (H&E) staining using reagents provided by Servicebio. Immunohistochemical staining for osteogenic marker OCN was performed as described previously [34]. IL-1β and IL-6 antibodies, as well as the secondary antibody (GB23303), were obtained from Servicebio. The sections were photographed with an Olympus CX31 microscope (Tokyo, Japan). The numbers of the IL-1β-, IL-6-, or OCN-positive cells were measured with the Image-Pro Plus 6 software.

Biomechanical test

Three-point bending tests were conducted on a mechanical testing machine (In-stron 3343, Canton, USA) to assess bone strength. Briefly, tibiae were positioned in the anterior–posterior direction (patella side facing up) on the lower supporting bars, spaced 8 mm apart. A constant vertical compression load (5 mm per minute) was applied to the midpoint of the samples until fracture occurred. The maximum bending load of the femur (N) was calculated from the load-displacement curve.

Isolation, identification, culture, and drug sensitivity of K. variicola

Fecal samples from the mice were collected following sterile procedures, then picked 1 g fecal samples inoculated on a blood agar and a MacConkey agar, cultured in 37℃ for 24 h. Organisms identification was performed using MALDI Biotyper (Bruker, Germany). *K. variicola* was cultured in LB broth (Solarbio, Beijing, China) with shaking (300 rpm) at 37 °C in a microaerophilic chamber (88% N2, 2% O2, 5% CO2, and 5% H2; LAI-3T; Shanghai Longyue Instrument Equipment Co. Ltd., Shanghai, China). The minimum inhibitory concentrations (MICs) of antimicrobial agents were analyzed by using a Vitek 2 Compact instrument (bioMérieux, France). E. coli strain ATCC 25,922 was used for quality control. Results were interpreted using the Clinical and Laboratory Standards Institute (CLSI) breakpoints for all the antimicrobial agents except tigecycline, which were interpreted using the European Committee on Antimicrobial Susceptibility Testing (EUCAST) breakpoints.

Preparation of K. variicola-EVs

For isolation of *K. variicola*-EVs, *K. variicola* were incubated in fresh LB broth for 3 days and then pelleted by sequential centrifugation at 2000 g for 30 min and 10,000 g for 30 min at 4 °C. The culture supernatant was filtered by a 0.22-μm filter (Millipore, Billerica, USA) and then concentrated 100-fold by centrifugation at 4000 g and 4 °C in Amicon Ultra-15 Centrifugal Filter Units (100 kDa; Millipore). *K. variicola*-EVs were purified from the concentrated supernatant using OptiPrep density gradient centrifugation. Briefly, *K. variicola*-EVs (1.33 ml per tube) were added at the bottom of OptiPrep solution [6.67 ml per tube; 60% (w/v) iodixanol; Sigma-Aldrich, St. Louis, USA] in a polyallomer Beckman Coulter tube (38.5 ml), thus producing a 50% OptiPrep layer. Solutions of 40% (8 ml), 20% (8 ml), and 10% (7 ml) OptiPrep and 1 ml of PBS were sequentially and carefully added on the 50% OptiPrep layer to generate a discontinuous gradient. After centrifugation for 18 h at 100,000 g with a SW 32 Ti rotor (k factor, 204), 2 ml each of the OptiPrep density gradient fractions was obtained for nanoparticle tracking analysis to determine the EV-rich fractions (fractions 12 and 13). The EV-rich fractions were diluted with PBS to 30 ml and subjected to centrifugation for 3 h at 100,000 g and 4 °C to pellet *K. variicola*-EVs. The obtained *K. variicola*-EVs were resuspended in PBS. A small volume of *K. variicola*-EVs was subjected to bacterial colony counting assay on LB agar plate to ensure that there is no bacterial contamination. Protein contents of *K. variicola*-EVs were tested using a Pierce BCA protein assay kit (Thermo Fisher Scientific). *K. variicola*-EVs were used immediately or stored at − 80 °C until downstream experiments.

Osteoclastic differentiation assay

RAW264.7 cells were seeded in a 48-well plate at a density of 1.5×10^4 cells per well and treated with 100 ng/ml RANKL, followed by stimulation with K. variicola-EVs or an equivalent volume of PBS. The negative control culture was cultivated in high-glucose DMEM supplemented with 10% FBS. Half of the medium was replaced every 3 days. After 6 days of induction, the cells were washed with PBS and fixed with 4% paraformaldehyde for 10 min. Following a wash with distilled water, the cells were stained for tartrate-resistant acid phosphatase (TRAP) using a commercially available kit (Sigma). TRAP + multinucleated cells (MNCs) with more than

three nuclei were identified as osteoclasts. The number of osteoclasts was enumerated using an inverted microscope (Leica).

qRT-PCR analysis

For fecal samples, total genomic DNA was extracted using the TIANamp stool DNA kit (Tiangen, Beijing, China). In the case of colon and cell samples, total RNA extraction was carried out using TRIzol reagent (Invitrogen, Carlsbad, CA). Following the assessment of total RNA purity and concentration, reverse transcription to cDNA was performed using the PrimeScript RT kit (Takara). Quantitative real-time polymerase chain reaction (qRT-PCR) was conducted using the TB Green Premix Ex Taq II (Takara). The 2^−ΔΔCT method was employed to calculate relative mRNA expression levels. Detailed primer sequences utilized in this study are provided in Supplementary Table 1.

Statistical analysis

Data are shown as means ± SD. Student's t test (unpaired, two-tailed) was used for analyzing the differences between two groups. Multiple-group comparisons were performed using one- or two-way analysis of variance (ANOVA) followed by Bonferroni post hoc test. $P < 0.05$ was considered statistically significant, with $^{*}P < 0.05$, $^{**}P < 0.01$, and $^{***}P < 0.001$.

Supplementary Information

The online version contains supplementary material available at https://doi.org/10.1186/s13099-025-00713-4.

Supplementary Material 1

Supplementary Material 2

Acknowledgements
We thank Dai Xinru for technical support in fecal 16 S rRNA sequencing.

Author contributions
XC: Investigation, Formal analysis, Visualization, Data Curation, Writing - original draft preparation. HML: Investigation, Formal analysis, Visualization, Data Curation, Writing-original draft preparation. GW: Conceptualization, Investigation, Visualization, Formal analysis. ZXW: Data Curation, Conceptualization, Investigation, Writing-Review & Editing. LY: Investigation, Visualization. HX: Conceptualization, Methodology, Writing-Review & Editing, Supervision, Project administration. SZ: Conceptualization, Methodology, Writing-original draft preparation, Writing-Review & Editing, Supervision, Project administration, Funding acquisition.

Funding
This work was supported by the [National Natural Science Foundation of China] under Grant [number 82402884], the [Hunan Province Natural Science Foundation of China] under Grant [number 2022JJ40854, 2024JJ5565], the [Youth Science Foundation of Xiangya Hospital] under Grant [number 2021Q07], and the [China Postdoctoral Science Foundation] under Grant [number 2023M733946].

Data availability
No datasets were generated or analysed during the current study.

Declarations

Ethics approval and consent to participate
Animal care and experimental procedures were supported by the Ethical Review Board at Xiangya Hospital of Central South University (ID number: 202005422).

Competing interests
The authors declare no competing interests.

Received: 14 January 2025 / Accepted: 15 May 2025
Published online: 07 June 2025

References

1. Sozen T, Ozisik L, Basaran NC. An overview and management of osteoporosis. Eur J Rheumatol. 2017;4(1):46–56.
2. Ensrud KE, Crandall CJ. Osteoporos Ann Intern Med. 2017;167(3):ITC17–32.
3. Pouresmaeili F, Kamalidehghan B, Kamarehei M, Goh YM. A comprehensive overview on osteoporosis and its risk factors. Ther Clin Risk Manag. 2018;14:2029–49.
4. Chinemerem Nwobodo D, Ugwu MC, Oliseloke Anie C, Al-Ouqaili MTS, Chinedu Ikem J, Victor Chigozie U, Saki M. Antibiotic resistance: the challenges and some emerging strategies for tackling a global menace. J Clin Lab Anal 2022, 36 (9), e24655.
5. Blaser MJ. Antibiotic use and its consequences for the normal Microbiome. Science. 2016;352(6285):544–5.
6. Castaneda M, Smith KM, Nixon JC, Hernandez CJ, Rowan S. Alterations to the gut Microbiome impair bone tissue strength in aged mice. Bone Rep. 2021;14:101065.
7. Schepper JD, Collins FL, Rios-Arce ND, Raehtz S, Schaefer L, Gardinier JD, Britton RA, Parameswaran N, McCabe LR. Probiotic Lactobacillus reuteri prevents postantibiotic bone loss by reducing intestinal dysbiosis and preventing barrier disruption. J Bone Min Res. 2019;34(4):681–98.
8. Yuan X, Zhou F, Wang H, Xu X, Xu S, Zhang C, Lu M, Zhang Y, Zhou M, Li H, Zhang T, Song J. Systemic antibiotics increase microbiota pathogenicity and oral bone loss. Int J Oral Sci. 2023;15(1):4.
9. Ramirez J, Guarner F, Bustos Fernandez L, Maruy A, Sdepanian VL, Cohen H. Antibiotics as major disruptors of gut microbiota. Front Cell Infect Microbiol. 2020;10:572912.
10. Lyu Z, Hu Y, Guo Y, Liu D. Modulation of bone remodeling by the gut microbiota: a new therapy for osteoporosis. Bone Res. 2023;11(1):31.
11. Zhang J, Lu Y, Wang Y, Ren X, Han J. The impact of the intestinal Microbiome on bone health. Intractable Rare Dis Res. 2018;7(3):148–55.
12. Lofmark S, Edlund C, Nord CE. Metronidazole is still the drug of choice for treatment of anaerobic infections. Clin Infect Dis. 2010;50(Suppl 1):S16–23.
13. Hernandez Ceruelos A, Romero-Quezada LC, Ruvalcaba Ledezma JC, Lopez Contreras L. Therapeutic uses of metronidazole and its side effects: an update. Eur Rev Med Pharmacol Sci. 2019;23(1):397–401.
14. Zimmermann P, Curtis N. The effect of antibiotics on the composition of the intestinal microbiota - a systematic review. J Infect. 2019;79(6):471–89.
15. Van Nel K, Matukane SR, Hamman BL, Whitelaw AC, Newton-Foot M. Effect of antibiotics on the human microbiome: a systematic review. Int J Antimicrob Agents. 2022;59(2):106502.
16. Patangia DV, Anthony Ryan C, Dempsey E, Paul Ross R, Stanton C. Impact of antibiotics on the human Microbiome and consequences for host health. Microbiologyopen 2022, 11 (1), e1260.
17. Liu J, Chen C, Liu Z, Luo Z, Rao S, Jin L, Wan T, Yue T, Tan Y, Yin H, Yang F, Huang F, Guo J, Wang Y, Xia K, Cao J, Wang Z, Hong C, Luo M, Hu X, Liu Y, Du W, Luo J, Hu Y, Zhang Y, Huang J, Li H, Wu B, Liu H, Chen T, Qian Y, Li Y, Feng K, Chen Y, Qi L, Xu R, Tang S, Xie H. Extracellular vesicles from child gut microbiota enter into bone to preserve bone mass and strength. Adv Sci (Weinh). 2021;8(9):2004831.
18. Villa CR, Ward WE, Comelli EM. Gut microbiota-bone axis. Crit Rev Food Sci Nutr. 2017;57(8):1664–72.
19. Sjogren K, Engdahl C, Henning P, Lerner UH, Tremaroli V, Lagerquist MK, Backhed F, Ohlsson C. The gut microbiota regulates bone mass in mice. J Bone Min Res. 2012;27(6):1357–67.
20. Surana NK, Kasper DL. Deciphering the tete-a-tete between the microbiota and the immune system. J Clin Invest. 2014;124(10):4197–203.

21. Nilsson AG, Sundh D, Backhed F, Lorentzon M. Lactobacillus reuteri reduces bone loss in older women with low bone mineral density: a randomized, placebo-controlled, double-blind, clinical trial. J Intern Med. 2018;284(3):307–17.
22. Sapra L, Dar HY, Bhardwaj A, Pandey A, Kumari S, Azam Z, Upmanyu V, Anwar A, Shukla P, Mishra PK, Saini C, Verma B, Srivastava RK. Lactobacillus rhamnosus attenuates bone loss and maintains bone health by skewing Treg-Th17 cell balance in Ovx mice. Sci Rep. 2021;11(1):1807.
23. Yan J, Charles JF. Gut Microbiome and bone: to build, destroy, or both?? Curr Osteoporos Rep. 2017;15(4):376–84.
24. Rios-Arce ND, Schepper JD, Dagenais A, Schaefer L, Daly-Seiler CS, Gardinier JD, Britton RA, McCabe LR, Parameswaran N. Post-antibiotic gut dysbiosis-induced trabecular bone loss is dependent on lymphocytes. Bone. 2020;134:115269.
25. Chadchan SB, Cheng M, Parnell LA, Yin Y, Schriefer A, Mysorekar IU, Kommagani R. Antibiotic therapy with metronidazole reduces endometriosis disease progression in mice: a potential role for gut microbiota. Hum Reprod. 2019;34(6):1106–16.
26. Nitzan O, Elias M, Peretz A, Saliba W. Role of antibiotics for treatment of inflammatory bowel disease. World J Gastroenterol. 2016;22(3):1078–87.
27. de Campos TA, de Almeida FM, de Almeida APC, Nakamura-Silva R, Oliveira-Silva M, de Sousa IFA, Cerdeira L, Lincopan N, Pappas GJ Jr., Pitondo-Silva A. Multidrug-Resistant (MDR) Klebsiella variicola strains isolated in a Brazilian hospital belong to new clones. Front Microbiol. 2021;12:604031.
28. Rodriguez-Medina N, Barrios-Camacho H, Duran-Bedolla J, Garza-Ramos U. Klebsiella variicola: an emerging pathogen in humans. Emerg Microbes Infect. 2019;8(1):973–88.
29. Zou C, Zhang Y, Liu H, Wu Y, Zhou X. Extracellular vesicles: recent insights into the interaction between host and pathogenic Bacteria. Front Immunol. 2022;13:840550.
30. Kim HY, Song MK, Gho YS, Kim HH, Choi BK. Extracellular vesicles derived from the periodontal pathogen Filifactor alocis induce systemic bone loss through Toll-like receptor 2. J Extracell Vesicles 2021, 10 (12), e12157.
31. Setiawan A, Widodo ADW, Endraswari PD. Comparison of Ciprofloxacin, Cotrimoxazole, and Doxycycline on Klebsiella pneumoniae: Time-kill curve analysis. Ann Med Surg (Lond). 2022;84:104841.
32. Potter RF, Lainhart W, Twentyman J, Wallace MA, Wang B, Burnham CA, Rosen DA, Dantas G. Population structure, antibiotic resistance, and uropathogenicity of Klebsiella variicola. mBio 2018, *9* (6).
33. Ruan Z, Yin H, Wan TF, Lin ZR, Zhao SS, Long HT, Long C, Li ZH, Liu YQ, Luo H, Cheng L, Chen C, Zeng M, Lin ZY, Zhao RB, Chen CY, Wang ZX, Liu ZZ, Cao J, Wang YY, Jin L, Liu YW, Zhu GQ, Zou JT, Gong JS, Luo Y, Hu Y, Zhu Y, Xie H. Metformin accelerates bone fracture healing by promoting type H vessel formation through Inhibition of YAP1/TAZ expression. Bone Res. 2023;11(1):45.
34. Rao SS, Hu Y, Xie PL, Cao J, Wang ZX, Liu JH, Yin H, Huang J, Tan YJ, Luo J, Luo MJ, Tang SY, Chen TH, Yuan LQ, Liao EY, Xu R, Liu ZZ, Chen CY, Xie H. Omentin-1 prevents inflammation-induced osteoporosis by downregulating the pro-inflammatory cytokines. Bone Res. 2018;6:9.

Publisher's note